

Interpolymer interaction in insulin-chitosan complexes

Irina Glazova, Larisa Smirnova, Olga Zamyshlyayeva, Sergey Zaitsev, Alexander Avdoshin, Vladimir Naumov & Stanislav Ignatov

To cite this article: Irina Glazova, Larisa Smirnova, Olga Zamyshlyayeva, Sergey Zaitsev, Alexander Avdoshin, Vladimir Naumov & Stanislav Ignatov (2019): Interpolymer interaction in insulin-chitosan complexes, *Supramolecular Chemistry*, DOI: [10.1080/10610278.2019.1614180](https://doi.org/10.1080/10610278.2019.1614180)

To link to this article: <https://doi.org/10.1080/10610278.2019.1614180>



Published online: 08 May 2019.



Submit your article to this journal [↗](#)



View Crossmark data [↗](#)

Interpolymer interaction in insulin-chitosan complexes

Irina Glazova, Larisa Smirnova, Olga Zamyshlyayeva , Sergey Zaitsev, Alexander Avdoshin, Vladimir Naumov and Stanislav Ignatov

Department of Chemistry, Lobachevsky State University of Nizhny Novgorod, Nizhny Novgorod, Russia

ABSTRACT

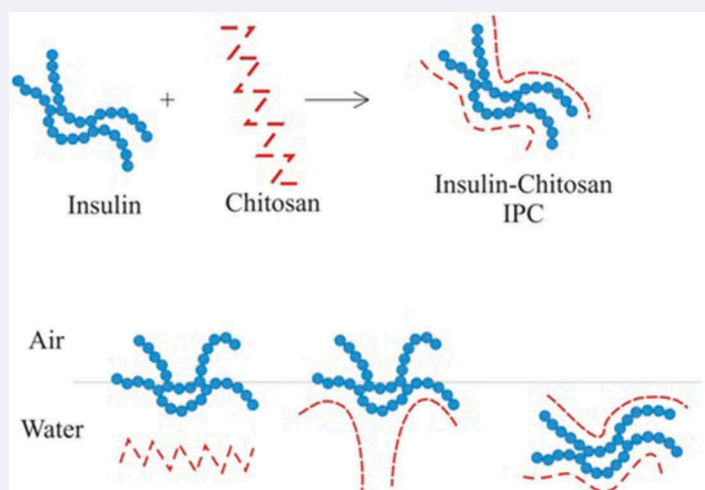
Our team conducted theoretical calculations and experimental studies of interpolymer interactions in insulin-chitosan complexes based on the spatial orientation of chitosan and insulin macromolecules using Langmuir film balance at various pH values. The most optimal conditions for interpolymer interactions between insulin and chitosan chains occur at pH value of 5.4, which corresponds to the isoelectric point of insulin. For the similar pH values of 4.2 and 6.0, the free energy of coordination between chitosan and insulin was estimated by molecular dynamic simulations as of 1.1 and 5.8 kcal mol⁻¹, respectively.

ARTICLE HISTORY

Received 13 February 2019
Accepted 28 April 2019

KEYWORDS

Chitosan; insulin;
interpolymer complexes;
molecular dynamics



Introduction

Insulin is a protein hormone produced in the pancreas by β -cells in islets of Langerhans. The main function of insulin is the enhancement of anabolic and inhibition of catabolic processes in muscles, liver, and fatty tissue. In particular, insulin increases the rate of synthesis of glycogen, fatty acids, proteins, and also stimulates glycolysis. Another very important function of insulin is the stimulation of the penetration of glucose, as well as a number of other sugars, and also amino acids into muscle cells and fatty tissue. By promoting the intake of glucose in these cells, the hormone reduces its content in the blood (1).

Since the discovery in 1922 by Baring and Best, insulin has been used as a medication for diabetes mellitus.

Diabetes is an endocrine disease that is determined by the absolute or relative insufficiency of the insulin hormone, resulting in hyperglycaemia – a persistent increase of glucose content in the blood. The main way to deliver the hormone is its injection. Disadvantages of this method of delivery include painful sensations and strict requirements to sterility.

According to the International Diabetes Federation, in 2011, the number of diabetes patients was 366 million, and by the year 2030, this number will reach 552 million (2). Therefore, possible alternative methods of hormone delivery are considered: peroral, rectal, nasal, etc. (3). This explains the growing professional interest in obtaining insulin-based drugs for oral administration. However, the introduction of insulin *per os* in its pure form does not render positive results,

since the protein is susceptible to the destructive effects of gastric acid (low pH values) and proteolytic enzymes of the gastrointestinal system.

In the light of the above, it is important to find the solution to the problem of protecting insulin molecules from the destructive action of enzymes and create conditions that ensure the effective infusion of the active component in the blood when administered *per os*. One promising solution in this regard is the synthesis of interpolymer complexes, in which the peptide molecules are shielded by layers of such a polymer, which, along with the protective function, would provide the transport of the hormone in the bloodstream (4).

The review article (5) provides data on natural and synthetic polymers used as templates for the delivery of insulin for oral use. Among the natural polymers there are chitosan and its derivatives, alginates, starch derivatives, polyesteramide and lysine derivatives (CS derivatives, alginate derivatives, poly- γ -glutamic acid-based materials, starch-based materials); among synthetic polymers there are derivatives of polyesteramide and lysine (synthetic polymers) polylactide, poly(lactide-co-glycolide, poly (ϵ -caprolactone)), L-Lysine-based poly (ester amide).

At the moment, in the attempts to create an oral form of insulin, scientists use various polymers, mostly natural. Among them, we can distinguish chitosan, dextran, alginate, poly(γ -glutamic acid), and hyaluronic acid. Less frequently used synthetic polymers include polylactide, polycaprolactone and acrylic polymers (6). In our view, chitosan appears to be the most promising element for the formation of interpolymer complexes with insulin, because it is biocompatible, biodegradable, non-toxic, and hydrophilic (7). Moreover, it has mucoadhesive and immunomodulating properties. Chitosan is a polycation, consisting of N-acetyl-D-glucosamine and D-glucosamine units. It is a deacetylated natural chitin polymer derivative. The authors (8) obtained chitosan nanoparticles containing insulin at pH 4 and determined the efficiency of association of the components using high-performance liquid chromatography. They have shown that the formation of complexes between insulin and chitosan occurs with a high degree of association under mild conditions.

Among the studies devoted to the preparation of polymer-insulin complexes for the oral administration of the latter, there are a few articles dedicated to establishing quantitative ratios of binding of components in the complex. Finding the proper ratios is extremely important for the development of multilayer systems with surface protection of the complex against premature release of insulin in the gastrointestinal tract. The paper (9) presents quantitative data on the binding of

insulin molecules to alkylated chitosan obtained using a wide range of physicochemical methods of investigation (Dynamic Light Scattering, NMR, IR spectroscopy and Isothermal Titration Calorimetry (ITC)).

However, the question of optimal conditions for the formation of such interpolymer complexes, in which the maximum interaction between insulin molecules and chitosan is achieved, remains open. The aim of this work was to study the behaviour of macromolecules of insulin and chitosan on the air-liquid interface and their intermolecular interactions on the Langmuir film balance. The monomolecular Langmuir layers obtained during the study serve as the most reliable and informative experimental data that allow studying conformational behaviour of amphiphilic molecules of a different nature at varying pH levels.

Experimental

Materials and methods

Materials

In our work, we used the pure insulin (authenticity 98.9%) provided by the Institute of Bioorganic Chemistry of the Russian Academy of Sciences. The test solutions with a concentration of 1 mg mL^{-1} were prepared by diluting the initial solution with deionized water. Different pH values were achieved by adding high-grade acetic acid and monitored using a pH meter (Mettler Toledo FEP20).

The studied solutions of chitosan (weight-average molecular weight = 200 kDa, polydispersity index = 1.46, deacetylation degree = 82%, produced by Bioprogress) with a concentration of 30 mg mL^{-1} were obtained by dissolution of chitosan in the 1.5% acetic acid. Changing the pH of chitosan solutions was carried out by adding NaOH.

The study of the properties of monomolecular layers of insulin, chitosan, and insulin-chitosan complexes

The influence of the pH medium on the confirmation of molecules was studied by the Langmuir automated balance (KVSMINI, Finland) with the platinum Wilhelmy plate. The surface area measurement error did not exceed 0.1%. The total surface area of the bath was 243 cm^2 . The water subphase was obtained using the deionized water with a resistivity index $c = 0.094 \text{ }\mu\text{Scm}^{-1}$, producing its pH values in the range from 4.7 to 6.2. The measurements were carried out at various volumes of a spreading solution. The surface pressure isotherms were obtained at a speed of barrier compression of 10 mm min^{-1} and constant $T = 24^\circ\text{C}$. Based on the obtained Langmuir isotherms, we determined the area occupied by all molecules of the monolayer by

extrapolation of the descending region of the isotherm $\pi = f(S)$, which corresponds to the formation of a “two-dimensional solid”. Surface area (a) per one macromolecule in the monolayer of insulin was determined by the formula:

$$a = \frac{S}{N} = \frac{S \cdot M}{C \cdot V \cdot N_a} \quad (1)$$

where N is the total number of molecules of insulin in the spreading solution, M is the molecular weight of insulin (mg mol^{-1}), C is the concentration of insulin in the spreading solution (mg mL^{-1}), N_a is the Avogadro's number, V is the volume of the spreading solution (mL), S is the surface area of all the insulin molecules (m^2).

We also calculated the elastic modulus of monolayers of insulin using the formula:

$$\varepsilon_0 = \frac{d\pi}{d \ln a} \quad (2)$$

where π – surface pressure (mN m^{-1}).

In the case of chitosan solutions, isotherms $\pi = f(S)$ were used to determine the coefficient of distribution of molecules between surface layer fluids and liquid subphase.

Chitosan-insulin complexes were obtained by mixing solutions of the corresponding components at pH 5.4. The ratios of chitosan and insulin by weight were 9:1; 3:1; 1:1, respectively. Using the isotherms $\pi = f(S)$ of these complexes we determined the surface areas of monomolecular square segments, which were then compared with calculated values based on the surface areas of molecules of individual components using the approximation of the absence of intermolecular interactions.

Determining the surface area of chitosan molecules at the liquid-gas interface at different pH values

The surface area per one chitosan molecule was calculated through the limiting adsorption value using the formula:

$$a = \frac{1}{G_\infty \cdot N_a} \quad (3)$$

The limiting adsorption value G_∞ was determined from the Langmuir equation through the values of adsorption. To find G we used the Gibbs equation. The values of the surface activity included in this equation were determined based on the isotherms of the surface tension of the corresponding solutions of chitosan. The surface tension of solutions of chitosan at the boundary with air was determined by the bubble pressure method on the Rebinder apparatus (10).

Molecular dynamics study of the chitosan-insulin coordination

In order to estimate thermodynamic data on the coordination of chitosan polymers on the insulin globules, the molecular dynamic (MD) study was carried out using the improved version of the 56A_{CARBO} force field (11). The 56A_{CARBO} is the high-accuracy force field applied for hydrocarbon calculations, which provides the proper description of the polyglycane chains in the aqueous solutions. Recently, it was modified in order to provide the proper description of the amino-glycane chains. The modified version of the force field, 56A_{CARBO_CHT} provides the good agreement with experimental data for the average angle distributions, NMR coupling constants, equilibrium rotamer distributions, as well as the proper description for the chitosan crystal dissolution process.

The model system consisted of two human insulin subunits coordinated on ZnCl_2 as presented in RSCB database (12) and surrounded by eight 10-monomer chains of chitosan (molecular mass of single polymeric chain is 1.6 kD). We used the cubic simulation box with 3D periodic boundary conditions. The box size was 10 nm. The simulation box was filled with the SPC water with randomly distributed Cl^- counterions providing electroneutrality of the system.

Structure of chitosan chains was generated from crystallographic data. The amino-groups of chitosan and ionogenic groups (amino and carboxyl) of insulin were protonated to simulate the pH influence of media using the experimental K_a of chitosan (13). Giving the known K_a , the number of ionized amino groups was determined unambiguously from pH values using the law of mass action. However, due to the microscopic nature of the model system, we can vary pH only in a step-wise manner.

The MD simulations were carried out for three pH values of 2.6, 4.2 and 6.0 for the NVT-ensemble at $T=300$ K, using the leap-frog integrator with LINCS bond constraint algorithm and the Berendsen thermostat. The simulation time was 30 ns with the integration timestep of 1 fs. The calculations were performed with the GROMACS v.5.0 software supporting CUDA accelerators at the Lobachevsky supercomputer facility of the University of Nizhny Novgorod.

Results and discussion

Properties of monolayers of insulin, chitosan and their complexes at the air-water interface

It is known that the main chemical and physical properties of solutions of polyelectrolytes, and the formation

of interpolymer complexes with their participation are largely determined by the spatial organization of molecules and significantly depend on the pH medium. Solving the task of determining the optimal conditions to ensure maximum availability of the functional groups of chitosan and insulin requires a study of the influence of pH medium on the dimensional characteristics of their molecules.

We studied the influence of pH medium on the insulin molecules orientation at the air-liquid interface at pH 4.7; 5.4; 6.2; which correspond to the states of the molecule before the isoelectric point, at the isoelectric point pI 5.4 and after. Obtained isotherms of surface pressure [π - S isotherm] (Figure 1) have a typical form for monolayers of polyampholytes, including proteins (14–16).

Since insulin is practically insoluble in water, we take its concentration in a monomolecular layer equal to its content in the volume of the spreading solution. The analysis of the curves and the corresponding calculations performed on their basis (Table 1) show that the insulin molecules occupy the largest surface area at the isoelectric point. It should be noted that this is contrary to the traditional behaviour of polyampholytes, the molecules of which in this state arrange into the most compact conformation. This can be explained by the structure of the insulin molecule. It consists of two polypeptide chains A and B connected by two disulphide bonds. The chain A consisting of 21 amino acid residues is water-soluble, has an internal disulphide bridge, and is negatively charged at pH 7. The B chain, containing 30 amino acid residues is

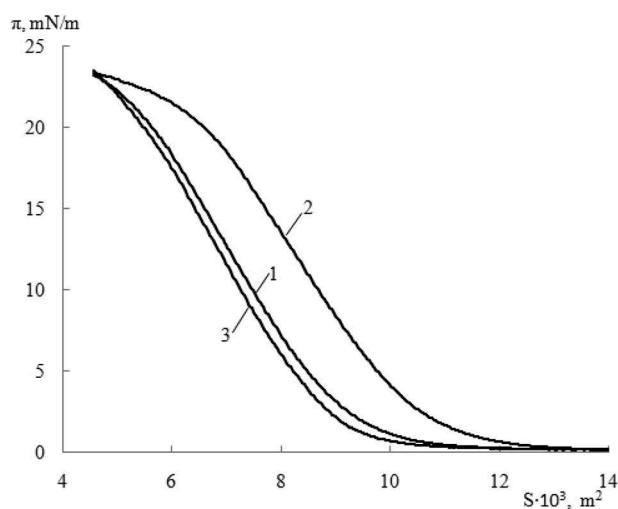


Figure 1. π - S isotherms of insulin monolayers compressed at various pH: 1–4.7; 2–5.4; 3–6.2 (concentration of the spreading solution = 1 mg mL⁻¹). $T = 24^{\circ}\text{C}$, π – surface pressure, S – surface area of all the molecules.

Table 1. Surface area (a) per one insulin macromolecule in the monolayer and the elastic modulus (ϵ_0) at varying pH.

pH	$a \cdot 10^{20}$, m ²	ϵ_0 , mN m ⁻¹
4.7	465	41.1
5.4	530	40.3
6.2	445	42.1

hydrophobic and becomes negatively charged only at a higher pH (17, 18). At the isoelectric point, when a molecule is neutral, the strongest interaction of the neutral functional groups of the two chains in a molecule occurs through hydrogen bonds. This makes the structure of the protein more rigid and shapes a spatial conformation, characterized by a higher magnitude. The MD simulations demonstrate that, at the isoelectric point of insulin (pH = 5.3–6.0), about 50% of chitosan monomeric units are coordinated at the insulin globule forming several hydrogen bonds (Figures 2–4). Among the formed H-bonds, two strongest ones are between the –OH group of chitosan and the –NH₂ group of arginine (Figure 5), and between the –OH group of chitosan and the oxygen of the asparagine (Figure 6). If the pH value deviates from pI to an acidic or alkaline medium, the amino acid chains in the protein acquire a charge; and due to the differences in composition, such an acquisition occurs unevenly.

The analysis of the IR transmission spectra (Figure 7) shows that the interaction between the components takes place equally over all possible bonds. Chitosan binding to insulin is possible according to the following functional groups: C–O–C (pyranose ring oxygen) and C–OH (1152 cm⁻¹, 2893 cm⁻¹), C(O)CH₃ and C–NH₂ (1385, 1696 and 1661 cm⁻¹). Insulin provides for the interaction of C–OH (1049 cm⁻¹), C(O)OH (1243, 1455 and 2963 cm⁻¹) and C(O)NH₂ (1455, 1538 and 1662 cm⁻¹). In the spectrum of the interpolymer complex, the positions of the characteristic bands of the

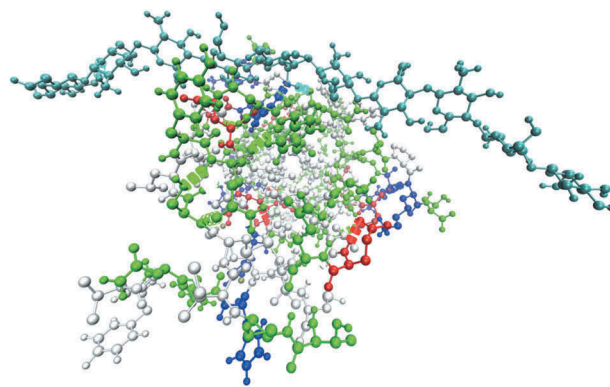


Figure 2. Coordination of chitosan chain at insulin globule after MD simulations at pH 6.

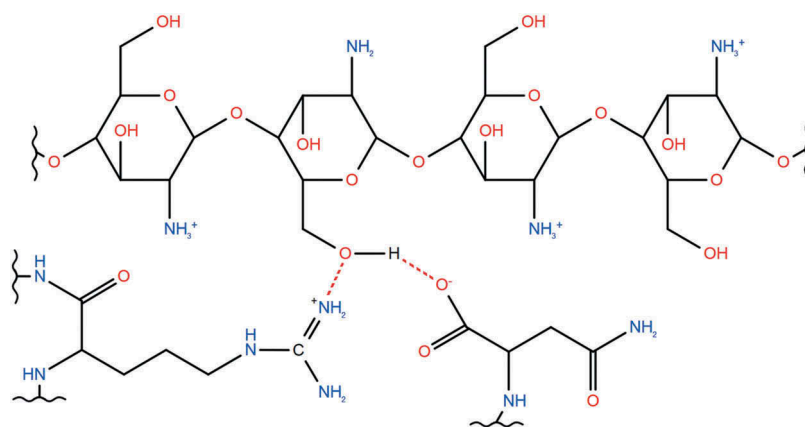


Figure 3. Scheme of formation of the strongest H-bonds between chitosan chain and insulin globule.

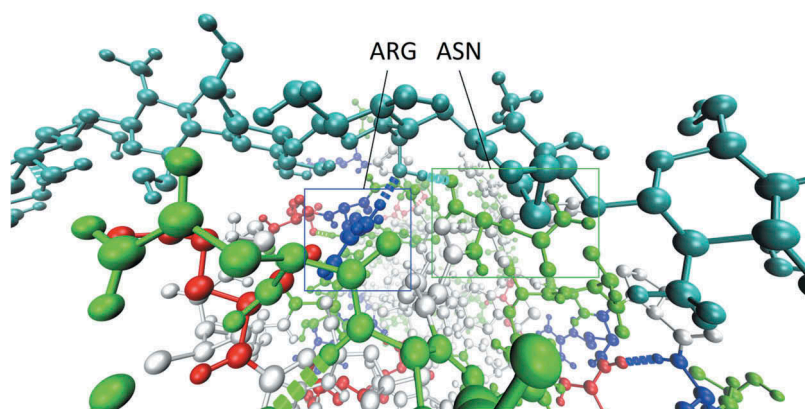


Figure 4. Two strongest H-bonds between the chitosan chain and insulin globule.

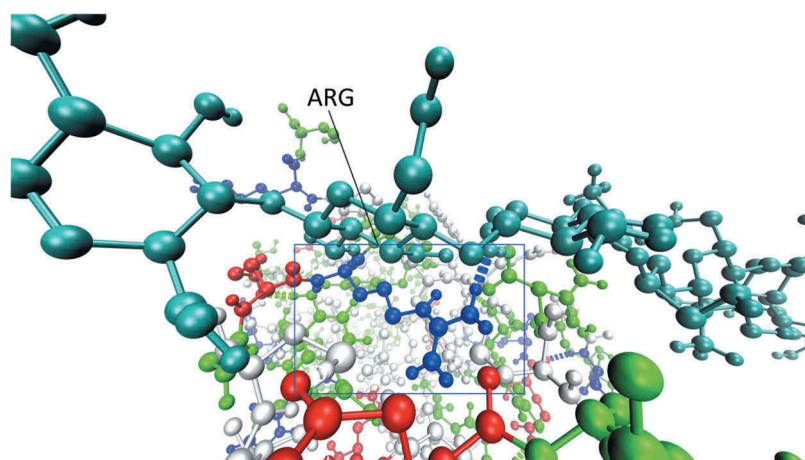


Figure 5. H-bond between chitosan and ARG residue of insulin.

pure components 1085, 1420, 1557, 1650, and 2928 cm^{-1} are shifted. This indicates the complexity of the process of binding insulin and chitosan in a complex and a presence of a variety of forces, among which the hydrogen bonds dominate.

The authors (19), who studied the mechanism of enzymatic action of Savinase on monomolecular layers of insulin, assume that this allows one chain to partially “push out” the second from the surface of the liquid phase to the gas phase, thereby reducing the surface

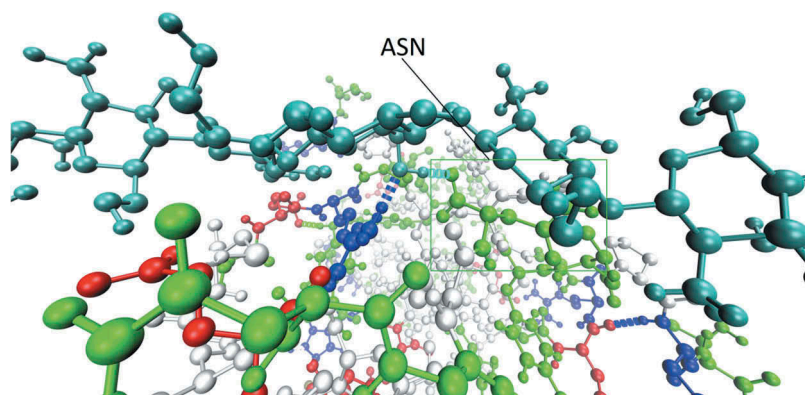


Figure 6. H-bond between chitosan and ASN residue of insulin.

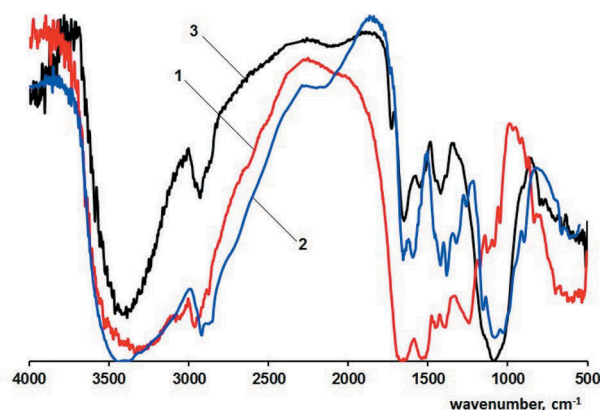


Figure 7. IR spectra of insulin (1), chitosan (2), and interpolymer complex insulin-chitosan (3).

area of the monolayer. The amino acid links pushed out of the surface into the air form loop structures, which leads to a spatial screening of the functional groups. The sterically inaccessible position of these groups leads to a decrease in the ability of insulin to form interpolymer complexes.

Based on the obtained Langmuir isotherms it is also possible to determine the elastic properties of monolayers (Table 1). It has been determined that the modulus of elasticity of insulin monolayers changes insignificantly against the variations of pH; however, it may be noted, that its minimum value is observed at the isoelectric point. This means that the monolayer has the loosest structure because of the minimal number of contacts between molecules. A slight increase in the modulus of elasticity, when the pH deviate from pI, is characteristic of the condensation of the monolayer structure due to intermolecular interaction associated with the attraction of oppositely charged functional groups and the dispersion interaction between hydrophobic regions of polymer chains.

Thus, the most favourable condition for the formation of interpolymer complexes of insulin is pH value = pI, when protein molecules have maximal extended conformations and interaction between its own molecules are minimal.

A similar complex of studies was carried out for solutions of chitosan. However, there was a problem of determining the concentration of chitosan in a monolayer, since its salt forms are highly soluble in water. To solve this problem, the Langmuir method was used to study the adsorption of chitosan from aqueous solutions at the boundary with air at varying pH.

The adsorption values of G at various pH values were calculated using the Gibbs equation:

$$G = - \frac{C}{RT} \frac{d\sigma}{dC} \quad (4)$$

using experimentally obtained surface tension isotherms (Figure 8), where C is the molar concentration and $-\frac{d\sigma}{dC}$ is the surface activity.

The dependence of the surface tension on the concentration was determined by the Rebinder method. Consequently, the C/G dependences were plotted against C (Figure 9). These dependencies were used in the Langmuir equation to calculate the value of the limiting adsorption G_{∞} and the surface area of the molecule of chitosan at various pH values (Table 2).

The obtained results show a significant dependence on the size characteristics of chitosan molecules on the pH medium. At pH values of 4.7, chitosan molecules have a more compact conformation, which can make it difficult to bind them to protein molecules. It is known (20) that, depending on the pH medium, chitosan macromolecules can have a coil or spiral conformation. It is the spiral conformation of the polysaccharide molecule that occurs when pH 5.4 is reached. Such an elongated structure enters into intermolecular

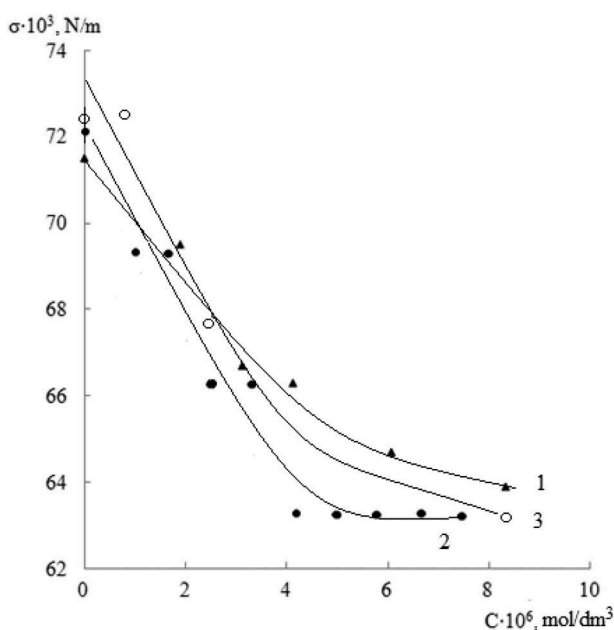


Figure 8. Isotherms of surface tension (σ) of chitosan water solutions at various pH: 1–4.7; 2–5.4; 3–5.8, $T = 24^\circ\text{C}$.

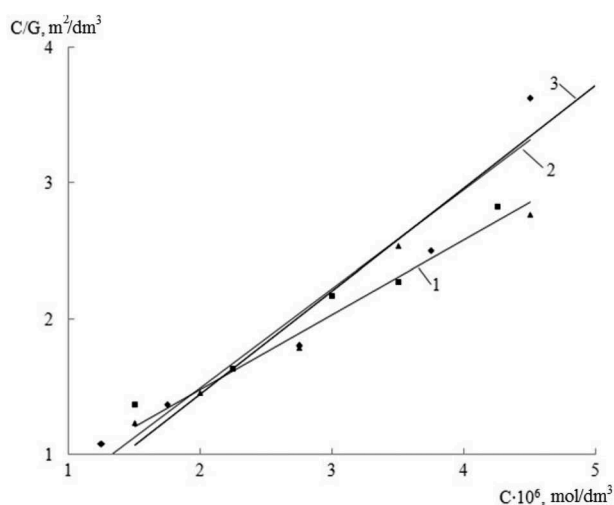


Figure 9. Dependence of C/G on the concentration of chitosan solutions (C) at various pH: 1–4.7; 2–5.4; 3–5.8 (G – adsorption).

Table 2. The limiting adsorption (G_∞) and surface area (a) per one chitosan macromolecule at the varying pH (tga – the angle of the line C/G on C from Figure 9).

pH	tga	$G_\infty \cdot 10^6, \text{mol m}^{-2}$	$a \cdot 10^{20}, \text{m}^2$
4.7	0.553	1.908	92
5.4	0.732	1.366	121
5.8	0.759	1.318	126

interaction with protein molecules much easier. Further increase of pH to 5.8 does not lead to significant changes in the surface area of the molecule; however, it is quite risky to work in this pH range, because this is

a boundary value corresponding to the loss of solubility of chitosan in water.

We used the obtained information about the area occupied by a molecule of chitosan to study the behaviour of monomolecular layers of chitosan at the air-liquid interface using the Langmuir balance and investigated the distribution of molecules of chitosan between bulk phase and surface coat. The obtained isotherms of monomolecular layers of chitosan at various pH-medium values are shown in Figure 10. In each of the cases considered, the volume of the spreading solution necessary for the formation of the monomolecular layer was different.

Our group defined the parameters, such as the area of a monolayer of chitosan molecules at the phase boundary (S, m^2), the number of molecules of chitosan at the phase boundary ($N_{\text{monolayer}}$), the number of molecules in the subphase (N_{subphase}) and distribution coefficient ($C_{\text{distribution}}$) of chitosan between the boundary layer and the volume of the water subphase (Table 3).

Despite the fact that at pH 4.7 and pH 5.4 monomolecular layers of chitosan have similar surface areas and almost identical distribution coefficient of molecules, volumes of the spreading solution necessary for the formation of monolayers differ significantly. At pH 4.7 this volume is greater, which allows to qualitatively estimate that the surface area per one chitosan molecule is smaller than its surface area at pH 5.4. The sharp increase in the surface area of the monolayer at pH 5.8 is not connected with an increase in the surface area per one molecule but with a decrease in the solubility of chitosan, manifested in an almost twofold increase of distribution coefficient of chitosan between the surface layer and the volume of subphase. As noted earlier, at

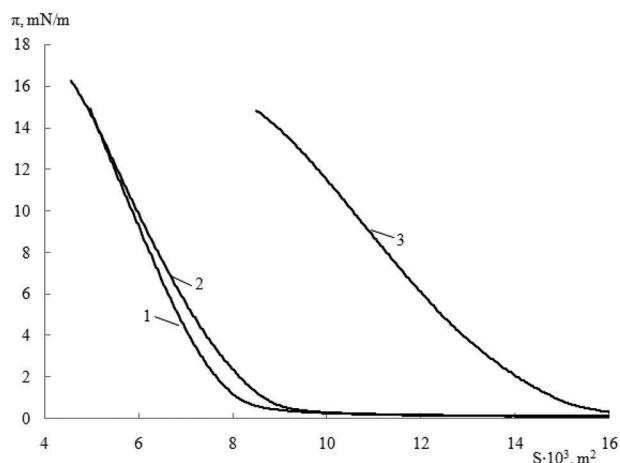


Figure 10. π - S isotherms of chitosan monolayers compressed at various pH: 1–4.7; 2–5.4; 3–5.8 (volumes of spreading solution: 1–520 μL ; 2–450 μL ; 3–400 μL), $T = 24^\circ\text{C}$.

Table 3. Characteristics of chitosan monolayers and distribution coefficient ($C_{\text{distr.}}$) between the interface and the volume of water subphase.

pH	$S \cdot 10^3, \text{m}^2$	$N_{\text{monolayer}} \cdot 10^{-15}$	$N_{\text{subphase}} \cdot 10^{-15}$	$C_{\text{distr.}} = \frac{N_{\text{monolayer}}}{N_{\text{subphase}}}, \%$
4.7	7.79	8.5	32.9	25.8
5.4	8.23	6.8	27.0	25.2
5.8	14.37	11.4	18.7	61.0

S is the area of a monolayer of chitosan molecules at the phase boundary; $N_{\text{monolayer}}$ is the number of molecules of chitosan at the phase boundary;

N_{subphase} is the number of molecules in the subphase;

$C_{\text{distr.}}$ is the distribution coefficient of chitosan between the boundary layer and the volume of the water subphase.

pH 5.8–6.0, chitosan in solution loses its stability and tends to precipitate.

Thus, the results obtained in the study of size variations of chitosan molecules by Langmuir isotherms confirm the aggregate data obtained from the study of Langmuir adsorption. This leads to the conclusion that the optimum conditions for forming interpolymer insulin-chitosan complex at pH 5.4, corresponding to pI of insulin, occur when both components have the longest conformations.

The formation of interpolymer chitosan-insulin complexes at pH 5.4 was carried out at different weight ratios of the components – 9:1, 3:1 and 1:1, respectively. For this purpose, we took a certain amount of pure insulin and added a calculated amount of 3% chitosan solution at pH 5.4. Then, we took the required amount of the spreading solution from the resulting mixture and conducted surface pressure measurements performed according to the procedure described above. The isotherms of interpolymer systems are shown in Figure 11.

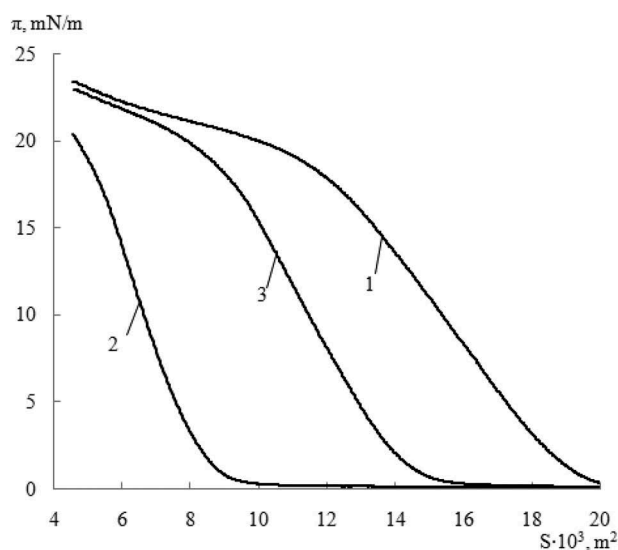


Figure 11. π - S isotherms of insulin-chitosan complex monolayers compressed at pH 5.4 with mass ratios: 1–9:1; 2–3:1; 3–1:1, $T = 24^\circ\text{C}$.

Based on Figure 11, we determined the experimental values of the surface area of monomolecular layers of various systems. In addition, based on the additive scheme, we calculated the areas of these systems, which they would occupy in the absence of interaction between insulin and chitosan. To do this, we used previously obtained data, such as the surface area of the insulin and chitosan molecules, and chitosan distribution coefficient at pH 5.4. Having calculated the exact content of the insulin in the original mixture, in the spreading solution, and the area occupied by one molecule at pH 5.4, we calculated the total area all protein molecules of the spreading solution would occupy on the phase boundary. Similarly, we calculated the area of the chitosan molecules on the basis of data on its concentration in the spreading solution, the distribution coefficient, and the area of one molecule (Table 4).

The comparison shows that in all the cases studied there is a significant deviation of the experimental values of the monolayer surface area from those calculated in the approximation of the absence of interaction between the molecules of insulin and chitosan. This confirms the formation of an interpolymer complex between the molecules of chitosan and insulin (Figure 12). In this case, the hydrophilic chitosan complexed with insulin “drags” the protein molecules from the surface into the water subphase, thereby reducing the total area of the monolayer. Moreover, the greatest changes occur in the 3:1 mixture, where apparently, the strongest bonding of components occurs.

Molecular dynamics study of the chitosan–insulin coordination

Within the simulation time, the coordination degree between insulin molecules and chitosan chains depends significantly on the pH value. At the end of simulation at the pH 2.6, only a single chitosan chain was coordinated with insulin globule with approximately 20% of monomers involved in coordination bonds. In the cases of pH 4.2 and 6.0, two or three chitosan chains were significantly coordinated, while additional chains interacted to the lesser degree. At higher pH values, from 4 to 8, chains interacted with insulin reaching the maximum coordination of all 8 chains at pH 7.5. This maximum coordination can be an occasional situation; however, it can also be the result of the competition between the chitosan-insulin and chitosan-chitosan coordination in alkaline media. In the cases of pH 9.3 and 10.1, five chains and seven chitosan chains, respectively, were coordinated at the insulin globule.

Table 4. Experimental and calculated values of different insulin-chitosan complexes of the monolayer areas.

Ratio	$S_{\text{exp}} \cdot 10^3, \text{ m}^2$	$S_{\text{calc}} \cdot 10^3, \text{ m}^2$	$\frac{S_{\text{exp}}}{S_{\text{calc}}}$	$S_{\text{insulin}} \cdot 10^3, \text{ m}^2$	$S_{\text{chitosan}} \cdot 10^3, \text{ m}^2$
9:1	19.20	31.2	0.615	30.88	0.32
3:1	8.36	80.3	0.104	80.03	0.28
1:1	14.23	64.6	0.220	64.53	0.07

S_{exp} - experimental values of insulin-chitosan complexes of the monolayer areas;

S_{calc} - calculated values of different insulin-chitosan complexes of the monolayer areas;

S_{insulin} - the area of the insulin molecules;

S_{chitosan} - the area of the chitosan molecules.

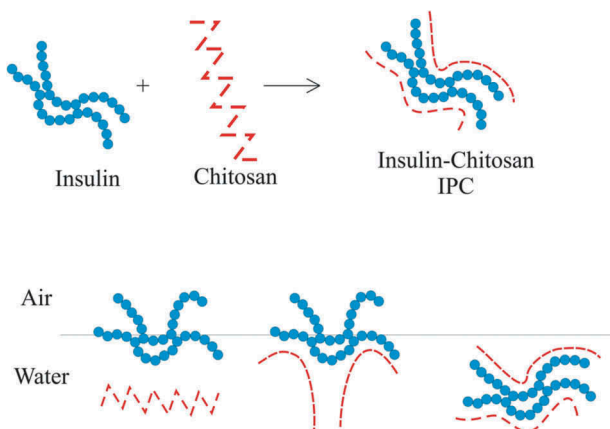


Figure 12. Scheme of formation of the insulin-chitosan interpolymer complex (IPC).

The insulin-chitosan coordination energy was estimated using the method of the potential of mean forces (PMF) and the umbrella sampling technique. The simulation box was extended to $10 \times 10 \times 20 \text{ nm}^3$. The starting system structures were taken from the previous free coordination MD runs using the single most coordinated chain of chitosan at the given pH (Figure 13). The umbrella potential consisted of 30 Gaussian functions with the heights of 6 kcal mol^{-1} and half-widths of 1.4 \AA placed at the 0.5 \AA intervals. Pulling force of $1000 \text{ kJ (mol/nm}^2\text{)}^{-1}$ was applied to the chitosan molecule. The final graph was obtained using the weighted histograms method with the default parameters (21–23).

During the pulling out, no significant changes in the insulin or chitosan conformations were observed as it can be seen in Figure 14.

Figure 15 shows the energy changes in the systems at different pH. The typical distance, when the coordination energy starts to increase, is about 1–1.5 nm. It should also be noted that the chitosan chains fall under the influence of other chitosan chains situated at the adjacent elongated simulation cells. These inter-cell interactions between charged chitosan chains can artificially increase the dissociation barrier making the estimated values somewhat overestimated. Thus, the final state of simulation corresponds to the approximate

value of dissolved chitosan concentration of 0.083 moles of chitosan chains per liter (0.83 mol L^{-1} of monomeric units) if we neglect the molar volume of insulin. The energy of insulin-chitosan coordination estimated as limiting values at high distances are $1.1 \text{ kcal mol}^{-1}$ for pH 4.2; $5.8 \text{ kcal mol}^{-1}$ for pH 6.0; $4.9 \text{ kcal mol}^{-1}$ for pH 7.5; $6.8 \text{ kcal mol}^{-1}$ for pH 9.3 and $13.4 \text{ kcal mol}^{-1}$ for pH 10. In the case of pH 2.6, there was no consistency in the PMF calculations, and only several distance points could be obtained resulting in apparent negative coordination energy value of about $-0.8 \text{ kcal mol}^{-1}$. This value should be considered as a preliminary estimate.

The dependence of the estimated values of insulin-chitosan coordination energy on the pH values is shown in Figure 16 (black circles). This dependence can be rationalized using the model, within which the interaction between chitosan and insulin molecules is described by the sum of Vander Waals interaction energy V (slightly dependent on pH) and Coulomb interaction energy linearly dependent on the charges of chitosan and insulin molecules Q_C and Q_I :

$$\Delta F = V + c \cdot Q_C Q_I \quad (5)$$

where c is a constant. The charges Q_C and Q_I strongly depend on pH in accordance with the Henderson-Hasselbalch equation. Assuming that the acid-base equilibrium of $\text{NH}_3^+/\text{NH}_2$ groups of chitosan is described by single apparent acidity constant pK_C , and the corresponding equilibrium of amino acids of insulin – by two constants pK_1 and pK_2 (for $-\text{COOH}$ and $-\text{NH}_2$ groups, respectively), the final expression of interaction energy has the form:

$$\Delta F = V + c \cdot \left(1 - (10^{pK_C - pH} + 1)^{-1} \right) \cdot \left(1 - (10^{pK_1 - pH} + 1)^{-1} - (10^{pK_2 - pH} + 1)^{-1} \right) \quad (6)$$

where V , c , pK_C , pK_1 , pK_2 are adjustable parameters. The non-linear fitting of these parameters gives the optimized values $V = 6.04 \text{ kcal mol}^{-1}$, $c = -7.84 \text{ kcal mol}^{-1}$, $pK_1 = 4.42$, $pK_2 = 9.59$, and $pK_C = 11$ (ΔF is only slightly dependent on pK_C when $pK_C > 11$). The resulting dependence is shown in Figure 16 with a solid red line. The optimized pK_C constants are somewhat higher than the

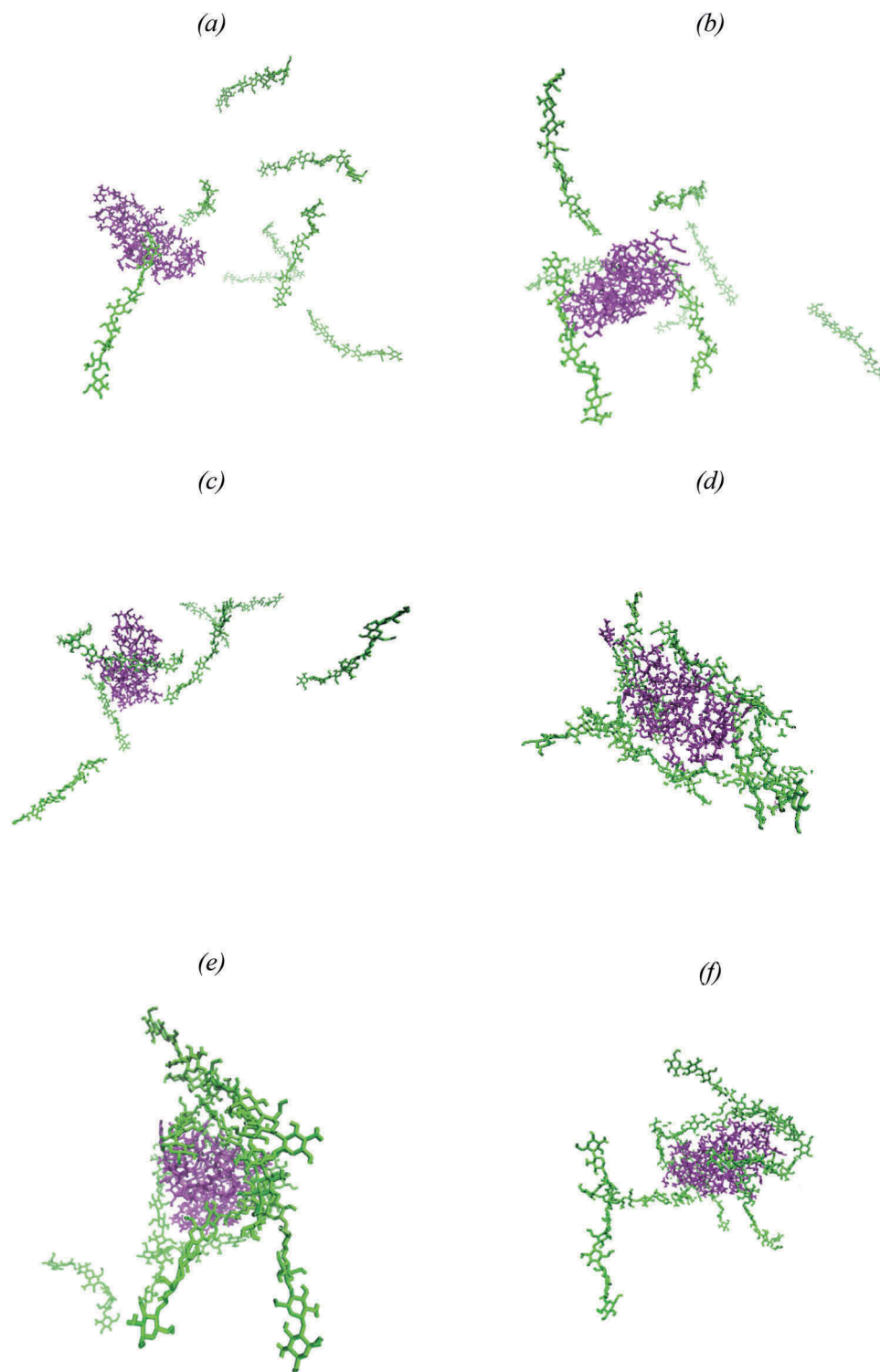


Figure 13. Chitosan–insulin interaction complexes after 30 ns simulations: (a) – pH 2.6; (b) – pH 4.2; (c) – pH 6.0; (d) – pH 7.5; (e) – pH 9.3; (f) – pH 10.0 Green chains – chitosan, purple globule – insulin.

experimental value of $pK_a = 8.35$ for $-NH_3^+$ group, and the corresponding pK_1 , pK_2 values are close to the typical acidity constants of different amino acids forming the insulin molecule. Thus, this qualitative model explains the basic features of the chitosan–insulin interaction found in the molecular dynamics simulations. In

a practice, the right part of the graph is inaccessible under the experimental conditions due to a strong association of chitosan at $pH > 9$.

The estimated values of the insulin–chitosan coordination free energy are in good agreement with the previous estimates made by experimental methods. In



Figure 14. Chitosan pulling from the insulin globule at pH 6.0.

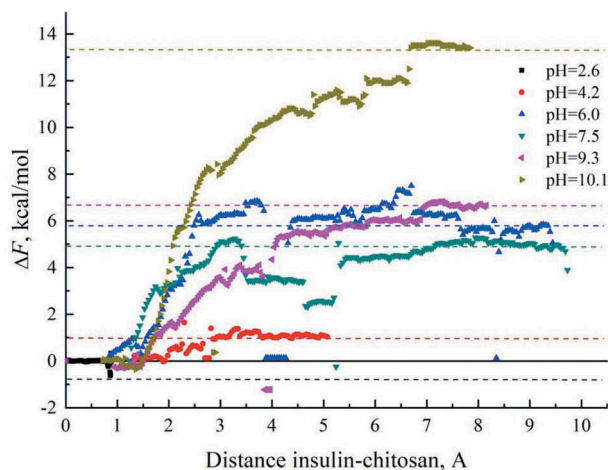


Figure 15. The estimated free Helmholtz energy (ΔF) of chitosan-insulin coordination at various pH.

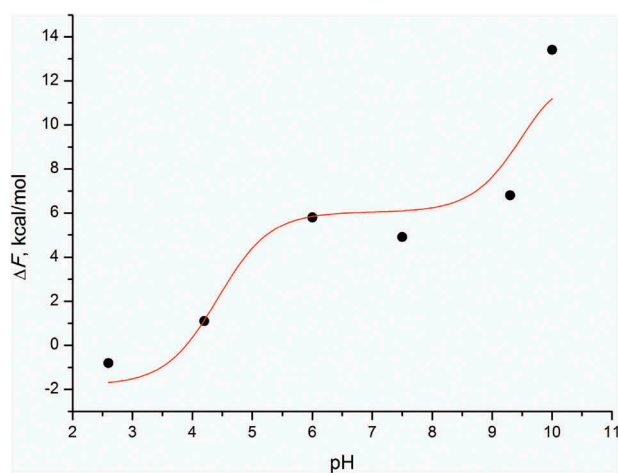


Figure 16. Dependence of the estimated free Helmholtz energy (ΔF) of the chitosan-insulin coordination on the pH values (black circles) and the fitted model (2) dependence taking into account the charges of chitosan and insulin molecules.

ref (9), the authors measured thermodynamic parameters of interaction between insulin with unmodified and hydrophobized chitosans at 5.3 pH and obtained the Gibbs free energy value of $3.03 \text{ kcal mol}^{-1}$. This value is in agreement with our value of $5.13 \text{ kcal mol}^{-1}$ resulting from the above regression formula at the experimental pH and taking into account the mean square discrepancy of the fitted values of about 3.3 kcal

mol^{-1} . The obtained regression dependence results in the coordination free energy values of $5.8\text{--}6.2 \text{ kcal mol}^{-1}$ slightly varied in the range of pH from 5.9 to 7.9. For the pH value of 5.4 which was found in the present study to be optimal for the insulin-chitosan coordination, the value of coordination free energy resulting from the regression dependence is of $5.30 \text{ kcal mol}^{-1}$. At the same time, the values directly estimated with the PMF calculations for the pH values of 4.2 and 6.0 (closest to the optimum) are of 1.1 and $5.8 \text{ kcal mol}^{-1}$, respectively.

Recently, the typical value of self-coordination energy of nanocrystalline chitosan consisting of 20-monomeric chains was estimated in the MD simulations with the same force field of about 44 kcal mol^{-1} (at protonation degree = 0), which was also in good agreement with the available experimental data (24). This value is much higher than insulin-chitosan coordination energy. Probably, this fact can explain the visually observed maximum of coordination between insulin and chitosan chains at pH 7.5 because at higher pH values the interaction between the chitosan chains located in different periodic cells prevails over the coordination at the insulin globule of the central cell.

Conclusions

The set of the obtained results allowed establishing the optimal conditions from the position of maximum interaction of insulin molecules with chitosan and the ratio of components ensuring complete binding of insulin to the complex (pH 5.4 and 3:1 by mass, respectively). The performed molecular dynamics simulations allowed us to obtain the dependence of the coordination free energy on the acidity of the medium in a broad range of pH values. The resulting dependence is in good agreement with the available experimental data and can be used for the prediction of insulin-chitosan coordination under various experimental conditions. The obtained data are necessary and can be used to create a multi-layered system on the basis of a structured insulin-chitosan complex with a protective coating of a biocompatible polymer that prevents insulin from the premature release into the gastrointestinal tract and increases the effectiveness of the drug for oral administration.

Acknowledgments

The authors are grateful to the Ministry of Education and Science of the Russian Federation (Project No 4.3760.2017/PCh). The MD simulations were performed using the supercomputer "Lobachevsky" of the University of Nizhny Novgorod.

Disclosure statement

No potential conflict of interest was reported by the authors.

Funding

This work was supported by the Ministry of Education and Science of the Russian Federation 4.3760.2017/PCh.

ORCID

Olga Zamyshlyayeva  <http://orcid.org/0000-0002-4331-3125>

References

- (1) Steiner, D.F. Biosynthesis of insulin. In Book Pancreatic Beta Cell in Health and Disease; Seino, S., Bell, G.I., Eds.; Springer: Japan, 2008; 31–49. <https://link.springer.com/content/pdf/10.1007%2F978-4-431-75452-7.pdf>
- (2) Whiting, D.R.; Guariguata, L.; Weil, C.; Shaw, J. IDF Diabetes Atlas: Global Estimates of the Prevalence of Diabetes for 2011 and 2030. *Diabetes Res.Clin.Pract.* **2011**, *94*, 311–321. DOI: [10.1016/j.diabres.2011.10.029](https://doi.org/10.1016/j.diabres.2011.10.029).
- (3) Kavimandan, N.J.; Peppas, N.A. Confocal Microscopic Analysis of Transport Mechanisms of Insulin across the Cell Monolayer. *Int. J. Pharm.* **2008**, *354*, 143–148. DOI: [10.1016/j.ijpharm.2007.12.014](https://doi.org/10.1016/j.ijpharm.2007.12.014).
- (4) Sonia, T.A.; Sharma, C.P. An Overview of Natural Polymers for Oral Insulin Delivery. *Drug Discovery Today.* **2012**, *17*, 784–792. DOI: [10.1016/j.drudis.2012.03.019](https://doi.org/10.1016/j.drudis.2012.03.019).
- (5) Luo, Y.Y.; Xiong, X.Y.; Tian, Y.; Li, Z.L.; Gong, Y.C.; Li, Y.P. A Review of Biodegradable Polymeric Systems for Oral Insulin Delivery. *Drug Delivery.* **2016**, *23*, 1882–1891. DOI: [10.3109/10717544.2015.1052863](https://doi.org/10.3109/10717544.2015.1052863).
- (6) Fonte, P.; Araujo, F.; Silva, C.; Pereira, C.; Reis, S.; Santos, H.A.; Sarmento, B. Polymer-Based Nanoparticles for Oral Insulin Delivery: Revisited Approaches. *Biotechnol. Adv.* **2015**, *33*, 1342–1354. DOI: [10.1016/j.biotechadv.2015.02.010](https://doi.org/10.1016/j.biotechadv.2015.02.010).
- (7) Muzzarelli, R.A.A. *Chitosan per Os: From Dietary Supplement to Drug Carrier*; Atec: Italy, 2001; pp 65–76.
- (8) Pan, Y.; Li, Y.J.; Zhao, H.Y.; Zheng, J.M.; Xu, H.; Wei, G.; Hao, J. S.; Cui, F.D. Bioadhesive Polysaccharide in Protein Delivery System: Chitosan Nanoparticles Improve the Intestinal Absorption of Insulin in Vivo. *Int. J. Pharm.* **2002**, *249*, 139–147. DOI: [10.1016/S0378-5173\(02\)00486-6](https://doi.org/10.1016/S0378-5173(02)00486-6).
- (9) Robles, E.; Juarez, J.; Burboa, M.G.; Gutierrez, L.E.; Taboada, P.; Mosquera, V.; Valdez, M.A. Properties of Insulin-Chitosan Complexes Obtained by an Alkylation Reaction on Chitosan. *J. Appl. Polym. Sci.* **2014**, *131*, 39999. DOI: [10.1002/app.39999](https://doi.org/10.1002/app.39999).
- (10) Birdi, K.S.; *Handbook of Surface and Colloid Chemistry*; 3; CRC Press Taylor and Francis Group: Boca Raton, 2009.
- (11) Hansen, H.S.; Hunenberger, P.H. A Reoptimized GROMOS Force Field for Hexopyranose-Based Carbohydrates Accounting for the Relative Free Energies of Ring Conformers, Anomers, Epimers, Hydroxymethylrotamers, and Glycosidic Linkage Conformers. *J. Comput. Chem.* **2011**, *32*, 998–1032. DOI: [10.1002/jcc.21675](https://doi.org/10.1002/jcc.21675).
- (12) Favero-Retto, M.P.; Palmieri, L.C.; Souza, T.A.; Almeida, F. C.; Lima, L.M. Structural Meta-Analysis of Regular Human Insulin in Pharmaceutical Formulations. *Eur. J. Pharm. Biopharm.* **2013**, *85*, 1112–1121. DOI: [10.1016/j.ejpb.2013.05.005](https://doi.org/10.1016/j.ejpb.2013.05.005).
- (13) Wang, Q.Z.; Chen, X.G.; Liu, N.; Wang, S.X.; Liu, C.S.; Meng, X.H.; Liu, C.G. Protonation Constants of Chitosan with Different Molecular Weight and Degree of Deacetylation. *Carbohydr. Polym.* **2006**, *8*, 194–201. DOI: [10.1016/j.carbpol.2006.01.001](https://doi.org/10.1016/j.carbpol.2006.01.001).
- (14) Nieto-Suarez, M.; Vila-Romeu, N.; Prieto, I. Behavior of Insulin Langmuir Monolayers at the Air-Water Interface under Various Conditions. *Thin Solid Films.* **2008**, *516*, 8873–8879. DOI: [10.1016/j.tsf.2007.11.062](https://doi.org/10.1016/j.tsf.2007.11.062).
- (15) Johnson, S.; Liu, W.; Thakur, G.; Dadlani, A.; Patel, R.; Orbulescu, J.; Whyte, J.D.; Micic, M.; Leblanc, R.M. Surface Chemistry and Spectroscopy of Human Insulin Langmuir Monolayer. *J. Phys. Chem. B.* **2012**, *116*, 10205–10212. DOI: [10.1021/jp3046643](https://doi.org/10.1021/jp3046643).
- (16) Liu, W.; Jonson, S.; Micic, M.; Orbulescu, J.; Whyte, J.; Garcia, A.R.; Leblanc, R.M. Study of the Aggregation of Human Insulin Langmuir Monolayer. *Langmuir.* **2012**, *28*, 3369–3377. DOI: [10.1021/la204201w](https://doi.org/10.1021/la204201w).
- (17) Nadendla, K.; Friedman, S.H. Light Control of Protein Solubility through Isoelectric Point Modulation. *J. Am. Chem. Soc.* **2017**, *139*, 17861–17869. DOI: [10.1021/jacs.7b08465](https://doi.org/10.1021/jacs.7b08465).
- (18) Sanger, F.; Thompson, E.O.P. The Amino-Acid Sequence in the Glycyl Chain of Insulin. 1. The Identification of Lower Peptides from Partial Hydrolysates. *Biochem. J.* **1953**, *53*, 353–366. DOI: [10.1042/bj0530353](https://doi.org/10.1042/bj0530353).
- (19) Balashev, K.; Ivanova, T.; Mircheva, K.; Panaiotov, I. Savinase Proteolysis of Insulin Langmuir Monolayers Studied by Surface Pressure and Surface Potential Measurements Accompanied by Atomic Force Microscopy (AFM) Imaging. *J. Colloid Interface Sci.* **2011**, *360*, 654–661. DOI: [10.1016/j.jcis.2011.04.101](https://doi.org/10.1016/j.jcis.2011.04.101).
- (20) Lyubina, S.Y.; Strelina, I.A.; Nudga, L.A.; Plisko, Y.A.; Bogatova, I.N. Flow Birefringence and Viscosity of Chitosan Solutions in Acetic-Acid with Various Ionic Powers. *Vysokomol Soed, A.* **1983**, *25(7)*, 1467–1472.
- (21) Wang, J.; Deng, Y.; Roux, B. Absolute Binding Free Energy Calculations Using Molecular Dynamics Simulations with Restraining Potentials. *Biophys. J.* **2006**, *91*, 2798–2814. DOI: [10.1529/biophysj.106.084301](https://doi.org/10.1529/biophysj.106.084301).
- (22) Souaille, M.; Roux, B. Extension to the Weighted Histogram Analysis Method: Combining Umbrella Sampling with Free Energy Calculations. *Comput. Phys. Commun.* **2001**, *135*, 40–57. DOI: [10.1016/S0010-4655\(00\)00215-0](https://doi.org/10.1016/S0010-4655(00)00215-0).
- (23) Hub, J.S.; de Groot, B.L.; van der Spoel, D. g_wham—A Free Weighted Histogram Analysis Implementation Including Robust Error and Autocorrelation Estimates. *J. Chem. Theory Comput.* **2010**, *6*, 3713–3720. DOI: [10.1021/ct100494z](https://doi.org/10.1021/ct100494z).
- (24) Avdoshin, A.A.; Ignanov, S.K. Determining the Thermodynamic and Kinetic Characteristic of Coordination of Chitosan Oligomers with Insulin using Methods of Molecular Dynamics. Presented at the Russian National Conference on Quantum and Mathematical Chemistry, Ufa, Russia, Nov 13, 2017.